Available online at www.sciencedirect.com
ScienceDirect
Coordination Chemistry Reviews 252 (2008) 336–346
COORDINATION CHEMISTRY REVIEWS
www.elsevier.com/locate/ccr

Review

Fourier transform infrared analysis of the photosynthetic oxygen-evolving center

Takumi Noguchi *

Institute of Materials Science, University of Tsukuba, Tsukuba, Ibaraki 305-8573, Japan

Received 28 February 2007; accepted 2 May 2007
Available online 6 May 2007

Contents

Abstract

Fourier transform infrared (FTIR) difference spectroscopy is a powerful method to study the detailed structures of active sites in enzymes. It can detect basically all molecules involved in trigger reactions and the structural information obtained is complementary to that by X-ray crystallography. Light-induced FTIR difference spectra of the photosynthetic oxygen-evolving center (OEC), which consists of the Mn_4Ca cluster embedded in photosystem II protein complexes, were obtained as spectral changes upon the first S_1-to-S_2 transition or during the S-state cycle. Band assignments were performed by isotopic substitution, quantum chemical calculations, and site-directed mutagenesis, while the structures and

Abbreviations: ATR, attenuated total reflection; DFT, density functional theory; FTIR, Fourier transform infrared; IR, infrared; OEC, oxygen-evolving center; PSII, photosystem II; Q_A, primary quinone electron acceptor; Y_Z, redox-active tyrosine on the D1 protein

* Tel.: +81 29 853 5126; fax: +81 29 853 4490.
E-mail address: tnoguchi@ims.tsukuba.ac.jp.

0010-8545/$ – see front matter
doi:10.1016/j.ccr.2007.05.001

reactions of OEC were analysed by applying certain perturbations on the OEC and detecting concomitant spectral changes. This review summarizes the FTIR studies on OEC thus far performed for understanding the molecular mechanism of photosynthetic oxygen evolution.

Keywords: FTIR; Infrared absorption; Mn cluster; Oxygen evolution; Photosystem II; S-state cycle

1. Introduction

Recent X-ray crystallographic studies of photosystem II (PSII) core complexes of thermophilic cyanobacteria revealed the structure of the oxygen-evolving center (OEC) to be a Mn_4Ca cluster ligated by several amino-acid ligands [1,2]. With the relatively low resolution of 3.0–3.5 Å and possible damage to the Mn cluster by X-ray radiation [3,4], however, the detailed OEC structure has not been resolved yet. In addition, inherent weakness of X-ray crystallography in detecting hydrogen atoms is a disadvantage in investigation of the mechanism of oxygen evolution, which is performed by four-electron oxidation of two water molecules involving proton release steps. Moreover, it is essential to detect the structures of all the metastable intermediates, called S states (S_0–S_3), in a light-driven reaction cycle (S-state cycle) of oxygen evolution. Such intermediate detection under physiological conditions is difficult to achieve by X-ray crystallography. Thus, some other spectroscopic methods, which cover the weakness of X-ray crystallography and provide complementary structural information, are necessary for full understanding of the molecular mechanism of photosynthetic oxygen evolution.

One of such spectroscopic methods is Fourier transform infrared (FTIR) spectroscopy. FTIR spectroscopy is one of vibrational spectroscopies, which detect the normal mode frequencies of molecular vibrations and reveals a molecular structure as an assembly of chemical bonds and interactions rather than as the positions of atoms. Thus, FTIR provides the information on the presence/absence and the strengths of certain chemical bonds or interactions, which is essential in understanding the molecular mechanisms of chemical reactions. Furthermore, FTIR is especially sensitive to protonation/deprotonation structures and hydrogen-bond interactions, which are the information often not available in X-ray crystallographic studies.

FTIR spectra of active sites of enzymes can be obtained using reaction-induced FTIR difference spectroscopy [5–7]. FTIR difference spectroscopy can detect signals from basically all molecules affected by a trigger reaction, including polypeptide main chains, amino acid side groups, cofactors, substrates, and water molecules. Thus, the spectra obtained contain a variety of information on the structures and reactions in the active sites. In contrast to FTIR, resonance Raman spectroscopy, which is another method to obtain vibrational spectra of active sites, is selective for specific vibrations of a cofactor coupled to its electronic transition at the excitation wavelength. However, the application of resonance Raman spectroscopy to the OEC have been limited to a few studies using the SERS (surface-enhanced Raman scattering) [8] and SERDS (shifted-excitation Raman difference spectroscopy) [9] techniques because of strong Raman scattering from a number of chlorophyll and carotenoid molecules in PSII samples. Careful analyses of the FTIR spectra using isotope substitution, quantum chemical calculations, site-directed mutagenesis, and so on provide information specific to a concerned molecule or a group in proteins. In addition, rather complex features of FTIR difference spectra in turn are useful as "fingerprints" to identify certain intermediates during enzymatic reactions.

The FTIR spectra of OEC were first reported in 1992 [10] as a difference upon the $S_1 \rightarrow S_2$ transition, which is the first transition by illumination on dark-adapted PSII sample, and spectra of all the flash-induced S-state transitions ($S_1 \rightarrow S_2$, $S_2 \rightarrow S_3$, $S_3 \rightarrow S_0$, and $S_0 \rightarrow S_1$) during the S-state cycle were obtained in 2001 [11,12]. During the past years, various analyses using this spectroscopy have been attempted and much information has been accumulated. This review summarizes the results of these FTIR studies. Readers may consult reviews of the same topic but more focused on low-frequency measurements by Chu et al. [13] and on measurement methods by Noguchi [14]. Also, a review of FTIR studies of redox-active cofactors of PSII including OEC by Noguchi and Berthomieu [15] may be consulted.

2. Detection of FTIR signals of OEC

FTIR signals of OEC are detected as absorption changes (typically, of the order of 10^{-4} or 10^{-5} as ΔA) by light-triggered reactions in membranes or core preparations of PSII. The most controllable reaction is the $S_1 \rightarrow S_2$ transition, which takes place by single-flash illumination on the dark-adapted PSII sample or by continuous illumination under conditions to ensure a single-turnover reaction. Successive flashes induce further S-state transitions (i.e., $S_2 \rightarrow S_3$, $S_3 \rightarrow S_0$, and $S_0 \rightarrow S_1$) in the S-state cycle and difference spectra upon individual flashes provide signals representing corresponding transitions.

2.1. S_1-to-S_2 transition

The first S_2/S_1 difference spectrum was detected by single-flash illumination on trypsin-treated PSII membranes of spinach in the presence of ferricyanide as an electron acceptor [10]. In this early work, trypsin treatment was adopted to facilitate electron abstraction at the electron acceptor side. However, it was later found that this treatment was not necessary and the spectrum was actually contaminated by signals of the non-heme iron, which was preoxidized by ferricyanide [16,17]. A pure S_2/S_1 spectrum was obtained using untreated PSII membranes in the presence of the ferricyanide/ferrocyanide (1:9) couple at 250 K [18]. In a relatively low pH buffer (pH 5.5) with a lower redox potential due to the high ferrocyanide ratio, the non-heme iron remained reduced, and hence the S_2/S_1 spectrum obtained contained no contamination of acceptor-side signals [17,18].

An alternative method to detect the S_2/S_1 signals without using artificial electron acceptors is measuring an $S_2Q_A^-/S_1Q_A$ difference spectrum by applying continuous illumination on PSII samples in the presence of DCMU or at cryogenic temperatures (~200 K) to block the electron transfer from Q_A to Q_B [10,19–24]. Subtraction of a Q_A^-/Q_A difference spectrum, which is obtained using Mn-depleted PSII in the presence of NH_2OH [25], from the $S_2Q_A^-/S_1Q_A$ spectrum provides an S_2/S_1 difference spectrum virtually identical to that using a ferricyanide/ferrocyanide couple [23,26,27]. An $S_2Q_B^-/S_1Q_B$ difference spectrum measured at room temperature using PSII membranes without DCMU was also reported [21].

Several different groups reported virtually identical S_2/S_1 or $S_2Q_A^-/S_2Q_A$ difference spectra [18,21–24,28,29] except for early work of one group, which showed significantly different spectra [30,31] perhaps due to a heat effect [20] and a high glycerol content (see footnote 2 in [28]). Two different forms of the S_2 states exhibiting the $g = 2$ multiline and $g = 4.1$ EPR signals were shown to have very similar FTIR signals, indicating that these two forms have only minor structural differences and are indistinguishable by molecular vibrations [20]. Recently, the S_2/S_1 difference spectrum of PSII membranes adsorbed on a silicon surface was measured using an ATR–FTIR technique [32], which will be useful for in situ detection of structural perturbations in OEC under different conditions.

2.2. S-state cycle

Chu et al. [33] applied two flashes to PSII OTG (octyl-β-D-thioglucopyranoside) cores at 250 K and obtained an S_3/S_2 difference spectrum by subtracting an S_2/S_1 spectrum by a single flash. The spectrum showed several bands absent in the S_2/S_1 spectrum. Hillier and Babcock [11] and Noguchi and Sugiura [12] independently measured the FTIR spectra during the S-state cycle by illumination of consecutive flashes. The former group used PSII membrane fragments from spinach and the latter used PSII core complexes from *Thermosynechococcus elongatus*. Despite the different PSII preparations and temperatures (265 K in the former versus 10 °C in the latter), spectral features at individual flashes were very similar between the two measurements.

Figs. 1 and 2 show flash-induced FTIR spectra of the S-state cycle in the mid-frequency (1800–1100 cm^{-1}) and high-frequency (3800–2200 cm^{-1}) regions, respectively, obtained using a moderately hydrated (or deuterated) film of core complexes from *T. elongatus* in the presence of ferricyanide as an exogenous electron acceptor [34,35]. The former region reflects the structural changes in the protein moiety comprising OEC and the latter region includes water OH (OD) vibrations in addition to protein bands (see below). Moderate hydration of a PSII film was achieved in a sealed IR cell in which a 20–40% glycerol/water (v/v) solution was placed without touching the sample [34]. The advantage of the film sample is that the strong IR absorption of bulk water in the regions of 3700–3000 (OH stretch) and 1700–1600 (HOH bend) cm^{-1} can be eliminated and sample stability is improved. The sample temperature was maintained at 10 °C. From the oscillation pattern of the peak

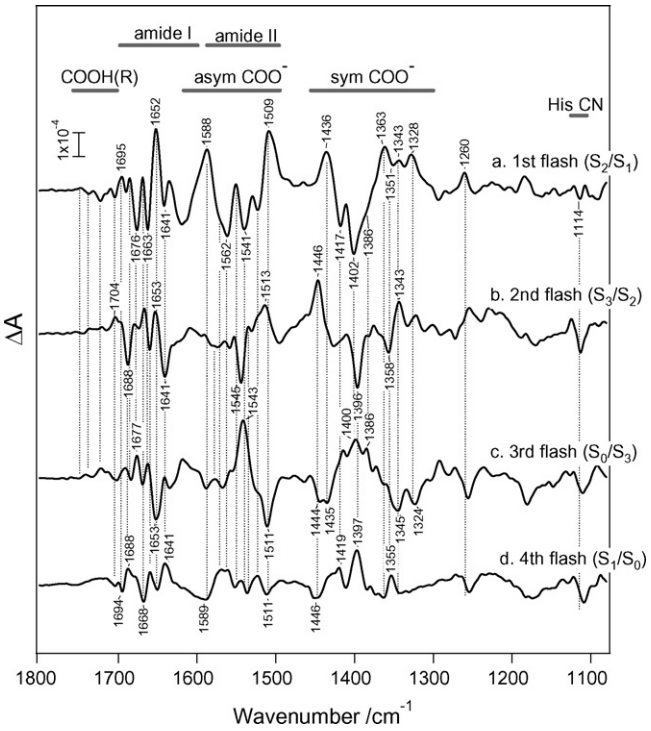

Fig. 1. Flash-induced FTIR difference spectra in the mid-frequency region (1800–1100 cm^{-1}) during the S-state cycle of OEC [34]. The sample was a moderately hydrated film of PSII core complexes from *Thermosynechococcus elongatus*. Difference spectra upon the 1st (a), 2nd (b), 3rd (c), and 4th (d) flashes represent the structural changes of OEC in the $S_1 \rightarrow S_2$, $S_2 \rightarrow S_3$, $S_3 \rightarrow S_0$, and $S_0 \rightarrow S_1$ transitions, respectively.

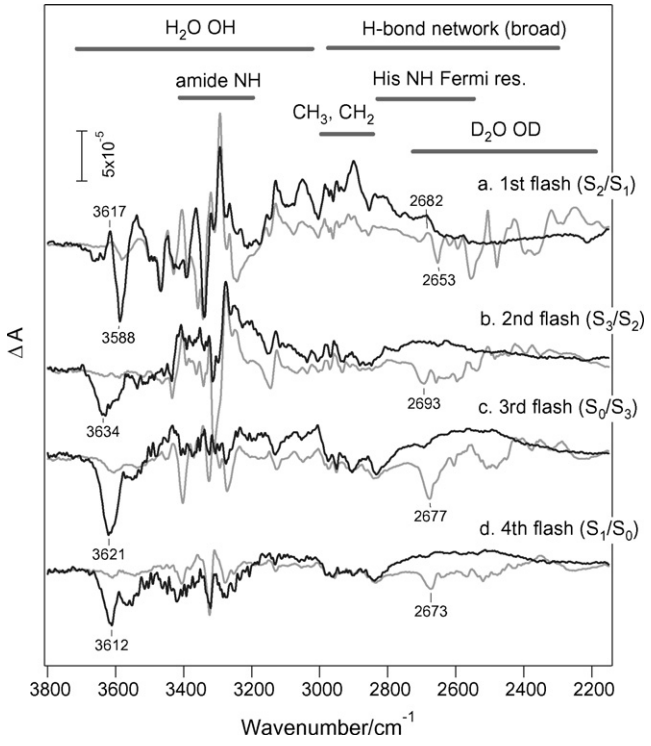

Fig. 2. Flash-induced FTIR difference spectra in the high-frequency region (3800–2200 cm^{-1}) during the S-state cycle of OEC [35]. The samples were moderately hydrated (black lines) and deuterated (gray lines) films of PSII core complexes from *T. elongatus* and the difference spectra were obtained upon the 1st (a), 2nd (b), 3rd (c), and 4th (d) flashes.

intensities, the miss factor was estimated as ∼12% [34]. Thus, spectra upon the 1st, 2nd, 3rd, and 4th flashes virtually represent the structural changes upon the $S_1 \rightarrow S_2$, $S_2 \rightarrow S_3$, $S_3 \rightarrow S_0$, and $S_0 \rightarrow S_1$ transitions, respectively. Although the second to fourth flash spectra include some contributions of other transitions, fifth to eighth flash spectra in the second cycle showed very similar features to the corresponding spectra in the first cycle [11,12], supporting that signals in the spectra mostly belong to the major transition. This situation of course depends on samples and measurement conditions, and when miss factors are large, spectra are severely distorted concomitant with decreased intensities especially after the 3rd flash. As shown in Fig. 1, most of the peaks in the 1st- and 2nd-flash spectra have counter peaks at the same frequencies but with opposite signs in the 3rd- or 4th-flash spectrum, indicating that the protein movements in the $S_1 \rightarrow S_2$ and $S_2 \rightarrow S_3$ transitions are mostly reversed in either the $S_3 \rightarrow S_0$ or the $S_0 \rightarrow S_1$ transition [12,34]. This characteristic of the S-state FTIR bands demonstrates well the catalytic role of the protein moieties comprising the OEC. However, the FTIR observation disagrees with the fact that oxidizing equivalents are accumulated in the $S_0 \rightarrow S_1 \rightarrow S_2 \rightarrow S_3$ transitions and then released in the $S_3 \rightarrow S_0$ transition to produce an oxygen molecule, indicating that protein movements do not necessarily correlate to the changes in the oxidation states of the Mn cluster.

3. Band assignments

Rough assignments of the S-state FTIR spectra can be achieved using the concept of group frequencies [36], in which individual chemical groups have their characteristic vibrational frequencies. The assignment of each group is supported by FTIR measurements of model compounds that have similar but simpler structures. In addition, quantum chemical calculations using, for example, the density functional theory (DFT) method, which has been used extensively for vibrational analysis, are quite powerful not only for band assignments but also for establishing criteria to obtain structural information such as protonation structures and hydrogen bond interactions. More accurate assignments should, however, be made by isotopic substitution, which is universally subjected to individual atomic species in proteins or ideally to specific atoms in amino acid residues or cofactors. Site-directed mutagenesis is useful to assign bands to a specific amino acid residue. Because of the secondary effects of mutation, however, minor spectral changes must be interpreted with caution as demonstrated by Strickler et al. [37].

3.1. Amide I and II bands of polypeptide backbones

All proteins show characteristic prominent bands at 1700–1600 and 1600–1500 cm^{-1}, which are due to the amide I (C=O stretch) and amide II (NH bend coupled with CN stretch) modes, respectively, of polypeptide backbones [38]. During enzymatic reactions, protein conformations are often perturbed and as a result amide I and II bands appear in reaction-induced FTIR difference spectra. In the spectra of the S-state cycle (Fig. 1), several prominent peaks are observed in the amide I (1700–1600 cm^{-1}) and amide II (1600–1500 cm^{-1}) regions. Most of the peaks at 1700–1600 cm^{-1} showed large downshifts by 40–50 cm^{-1} upon universal ^{13}C labeling and slight downshifts by a few wave numbers upon ^{15}N labeling, and thus they were assigned to the amide I modes [18,39–42]. Amide I frequencies reflect polypeptide conformations [38]. The presence of several intense amide I peaks in a relatively wide range in 1700–1600 cm^{-1} indicates that different polypeptide conformations coexist in the protein moiety comprising OEC, which is consistent with the recent X-ray structures [1,2]. Rather different band features between the 1st- and 2nd-flash spectra indicate that different polypeptide chains are perturbed between the $S_1 \rightarrow S_2$ and $S_2 \rightarrow S_3$ transitions. The former change seems to be reversed mostly in the $S_3 \rightarrow S_0$ transition, while the latter in the $S_0 \rightarrow S_1$ transition (Fig. 1).

Some of the peaks in the 1600–1500 cm^{-1} region, for example, peaks at 1545–1541 cm^{-1} showed moderate downshifts by 10–20 cm^{-1} both upon ^{13}C labeling and ^{15}N labeling [18,39–42]. Thus, they were assigned to the amide II modes of backbone amides, which are coupled to the amide I peaks.

3.2. Carboxylate groups

The most striking features of the FTIR difference spectra of OEC are several prominent peaks in the typical asymmetric and symmetric carboxylate stretching regions at 1600–1500 and 1450–1300 cm^{-1}, respectively (Fig. 1). Indeed, all the major bands in the 1450–1300 cm^{-1} region underwent large ^{13}C downshifts by 25–45 cm^{-1} without any ^{15}N shifts [18,39–42] (acetate in aqueous solution showed ^{13}C downshifts by 42 and 26 cm^{-1} in the asymmetric and symmetric vibrations, respectively [40]). Hence, these bands were assigned to the symmetric COO^- stretching modes originating from Asp, Glu, or the C-terminus. Since no other prominent bands interfere with this region, the symmetric COO^- bands can be good monitors of the structures and reactions of carboxylate groups coupled to the Mn cluster. On the other hand, the asymmetric COO^- bands at 1600–1500 cm^{-1} severely overlap the amide II bands, and thus the assignments are not straightforward. However, some peaks, for example, at 1588, 1562, and 1513–1509 cm^{-1} (Fig. 1), showed large downshifts by 30–50 cm^{-1} upon universal ^{13}C labeling without any ^{15}N shifts, and thus these were assigned to the asymmetric COO^- vibrations [18,39–42].

The absence of prominent peaks at 1760–1700 cm^{-1}, where the C=O stretches of COOH groups typically show bands [36], indicates that the prominent COO^- bands in the S-state spectra do not originate from protonation/deprotonation reactions of COO^-/COOH groups, but rather arise from structural perturbations of COO^- groups during the S-state cycle. It is most likely that carboxylate ligands to the Mn_4Ca cluster change their coordination structures and bond orders. In the symmetric COO^- region of the four flash-induced spectra (Fig. 1), about 10 corresponding peaks are recognized at different frequencies, suggesting that several carboxylate groups are coupled with the Mn cluster. This seems consistent with the X-ray structure of OEC, in which six carboxylate groups (D1-Asp170, D1-Glu189, D1-Glu333, D1-Asp342, α-COO^- of D1-Ala344, and CP43-Glu354) are found in the close vicinity of the Mn or Ca ions [1,2].

Attempts to assign the COO^- bands to specific residues have been made using site-directed mutagenesis and selective isotope substitution. Chu et al. [28] showed that the symmetric stretching bands of the α-COO^- group of D1-Ala344 exist at ∼1356 cm^{-1} in the S_1 state and at ∼1339 or ∼1320 cm^{-1} in the S_2 state in the PSII particles of *Synechocystis* sp. PCC 6803, using combination of L-[1-^{13}C]alanine labeling and D1-Ala344Gly and D1-Ala344Ser mutations. Kimura et al. [43] further reported that the D1-Ala344 signal at the 1st flash was mostly reversed at the 3rd flash. On the other hand, D1-Asp170His [44,45] and D1-Asp342Asn [46] mutations did not alter the COO^- stretching bands in any flash-induced transitions. Kimura et al. [47] observed that symmetric COO^- bands at 1450–1370 cm^{-1} in the S_2/S_1 spectrum were slightly perturbed by Glu189Gln mutation and proposed that the bands of Glu189 exist in this region. However, Strickler et al. [37] showed that neither the Gln nor Arg mutations at D1-Glu189 eliminates any COO^- stretching bands and small spectral alterations were similar in amplitude to those by different methods of sample handling or mutation at a residue that is located apart from the Mn cluster. Thus, these mutagenesis studies showed that at least three out of the six putative carboxylate ligands are silent in S-state FTIR spectra. This is rather controversial to the presence of about 10 corresponding peaks in the symmetric COO^- region (see above). This discrepancy has to be resolved by definite assignments of bands in future works.

The minor peaks in the 1760–1700 cm^{-1} region are attributable to the C=O stretching vibrations of COOH groups [40] or ester C=O groups of chlorophylls. These groups may be structurally or electrostatically coupled to the Mn cluster and slightly perturbed by S-state reactions. The peaks were virtually unaffected in a deuterated film [35]. Thus, if they arise from COOH groups, they must exist in hydrophobic environments but not in proton or water pathways between OEC and the lumenal side.

3.3. Histidine

The imidazole group of His exhibits a characteristic CN stretching band at around 1100 cm^{-1}, which is sensitive to protonation structures and a good marker of His structures [16,48–53]. In the S_2/S_1 spectrum, a negative peak was observed at 1114–1113 cm^{-1} and downshifted by ∼7 cm^{-1} upon both universal ^{15}N labeling and selective ^{15}N-imidazole labeling (Fig. 3B) [42,49,54]. Thus, this peak was assigned definitely to the vibration of a His side chain. The criterion to identify the protonation structures of a His side chain was determined by FTIR measurements of model compounds (4-methylimidazole and DL-histidine) [48–50] and quantum chemical calculations [50–53]. This criterion was shown to be applicable to metal complexes by DFT calculation [51] as well as by examples of bis(4-methylimidazole) complex of iron protoporphyrin [48], and Cyt*b*559 [48] and the non-heme iron [16] in PSII. From the peak frequency at 1114–1113 cm^{-1} together with insensitivity to D_2O exchange, it was proposed that the His in OEC takes a neutral imidazole form protonated at the Nπ site, and hence coordinated to Mn at the Nτ site (Fig. 3C) [49]. In addition, several Fermi resonance peaks of a hydrogen-bonded NH stretching vibration were observed at 2850–2500 cm^{-1} (Fig. 3A), which indicated that the NH group of the observed His is hydrogen bonded [49] (Fig. 3C). The most likely candidate for this His is D1-His332, which ligates a Mn ion at the Nτ site, and its NπH is within a hydrogen-bonding distance of the backbone C=O of D1-Glu329 in the X-ray structures [1,2]. The possibility of D1-His337, which is also located in the vicinity of the Mn cluster, cannot be excluded at present. Kimura et al. [54] identified His CN bands during the S-state cycle by universal ^{15}N labeling and L-[$^{15}N_3$]His labeling, and reported that the His vibration was mainly perturbed in the $S_1 \rightarrow S_2$, $S_2 \rightarrow S_3$, and $S_0 \rightarrow S_1$ transitions but not in the $S_3 \rightarrow S_0$ transition.

3.4. Low-frequency vibrations of the Mn cluster core

The low-frequency region below 1000 cm^{-1} contains vibrations of the Mn cluster core and metal-ligand bonds [13]. The vibrations of [Mn(μ-O)]$_2$ cores (700–600 cm^{-1}), Mn–OH_2 (500–200 cm^{-1}), $Mn^{V \text{ or } IV}$=O (1000–700 cm^{-1}) are expected to be observed in the OEC spectra [13]. Chu et al. [22] first obtained the S_2/S_1 difference spectra in the low-frequency region (<1000 cm^{-1}) by using window materials, a beam splitter, a detector, and a band-pass filter suitable for low-frequency measurements [55,56]. They found that the bands at 606/625 cm^{-1} downshifted by about 10 cm^{-1} in $H_2{}^{18}O$, but were not affected by $^{44}Ca^{2+}$ substitution; thus, these bands were assigned to a Mn–O–Mn cluster vibration of OEC [57]. The assignments to the Mn–O–Mn or Mn–O stretching vibrations were supported by ATR–FTIR measurements of adamantane-like Mn compounds in two different oxidation states (Mn_4^{IV} and $Mn^{III}Mn_3^{IV}$) [58] and vibrational analyses of model Mn complexes by the GF-matrix method [58,59] or the DFT method [60]. Visser et al. [58] suggested that two bands at 606/625 cm^{-1} (S_2/S_1) are not the same vibrational modes and are from different symmetry representations. Chu et al. [61] found Mn–O–Mn vibration in the S_3 state at ∼621 cm^{-1} by two-flash experiments. Low-frequency S_2/S_1 spectra using universally ^{15}N- or ^{13}C-labeled PSII core complexes showed that most of the low-frequency bands were derived from vibrational modes coupled with nitrogen- and/or carbon-containing groups [41].

Low-frequency spectra during the S-state cycle were reported by Kimura et al. [62] and analyzed using isotope-labeled water ($H_2{}^{18}O$, $D_2{}^{16}O$, and $D_2{}^{18}O$). Several bands sensitive to both $^{16}O/^{18}O$ and H/D exchanges were found at 670–540 cm^{-1} and attributed to the structure involving Mn and oxygen coupled with hydrogen. The possible origin of these bands was proposed to be water-derived intermediate associated with the Mn cluster [62]. In resonance Raman spectra of OEC with 820-nm excitation, Cua et al. [9] found four D_2O-sensitive bands at 500–300 cm^{-1}, which were attributed to Mn–OH_2 or Mn–OH vibrations. However, only minor bands were found below 500 cm^{-1} in FTIR difference spectra [62] and thus the corresponding IR bands have not been identified yet.

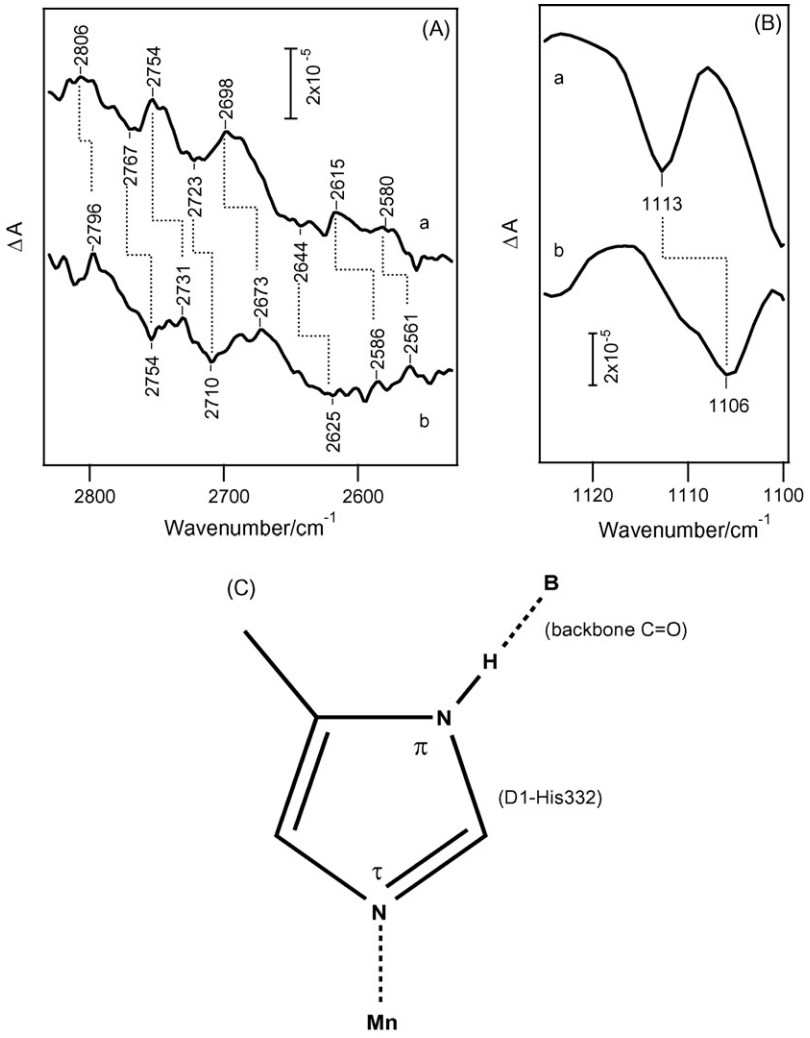

Fig. 3. S_2/S_1 difference spectra in the hydrogen-bonded NH stretching region (A) and the CN stretching region (B) of the imidazole side chain of His [49]. The samples were PSII core complexes from unlabeled *Synechocystis* sp. PCC 6803 cells (a) and cells in which two imidazole nitrogen atoms of His were selectively labeled with ^{15}N (b). (C) The structure of a His ligand proposed by FTIR spectra. A hydrogen bond acceptor is expressed as B. The most likely candidate of this His ligand is D1-His332 that is hydrogen-bonded with the backbone C═O of D1-Glu329.

3.5. Water OH vibrations and signals of hydrogen bond networks

The OH stretching vibrations of water molecules in OEC were first detected in the S_2/S_1 spectrum in the weakly hydrogen-bonded OH region (3700–3500 cm^{-1}) using the core complexes from *T. elongatus* at 250 K [63]. A wider water OH(OD) region during the S-state cycle was measured using a hydrated (deuterated) film of PSII core complexes [35] (Fig. 2). Assignments of the water OH(OD) vibrations were made by $H_2{}^{18}O$ ($D_2{}^{18}O$) substitution [35,63]. In the $S_1 \rightarrow S_2$ transition, a differential signal at 3617/3588 cm^{-1} (2682/2653 cm^{-1} in D_2O) was observed, whereas the $S_2 \rightarrow S_3$, $S_3 \rightarrow S_0$, and $S_0 \rightarrow S_1$ transitions showed negative OH bands at different frequencies at 3634, 3621, and 3612 cm^{-1} (2693, 2677, and 2673 cm^{-1} in D_2O) in the weak hydrogen-bond region. These negative bands indicate either proton release reactions or the formation of strong hydrogen bonds. Strongly hydrogen-bonded OD bands of D_2O during the S-state cycle, which were detected as double difference spectra between the spectra in $D_2{}^{16}O$ and $D_2{}^{18}O$, exhibited broad features in the range of 2600–2200 cm^{-1} [35].

On the lower-frequency side of water OH region, broad continuum features were observed around 3000, 2700, 2550, and 2600 cm^{-1} in the 1st, 2nd, 3rd, and 4th flash spectra, respectively [35] (Fig. 2). These broad features probably arise from high proton polarizability in hydrogen bonds [64]. Thus, band appearances in the S-state spectra and different maximum positions among the S-state transitions may reflect changes in the hydrogen-bond networks around OEC in the course of water oxidation.

3.6. Other vibrations

Relatively sharp peaks were observed in the high-frequency region of 3450–3250 cm^{-1} in the S-state spectra of hydrated or deuterated PSII films of *T. elongatus* [35,40] (Fig. 2; the lower S/N in a hydrated film is due to absorption of bulk water). These bands were downshifted by 6–15 cm^{-1} upon universal ^{15}N sub-

stitution but unaffected upon ^{13}C substitution, and thus assigned to the NH stretching bands of backbone amides [40]. The observation that these bands were mostly left in a deuterated film indicates that a large portion of the polypeptide main chains coupled to the OEC reactions is in rather hydrophobic environments [35,40].

Using the *Synechocystis* sp. PCC 6803 cores labeled with [ring-4-^{13}C]Tyr, the signals of a tyrosine side chain in the S_2/S_1 spectrum were identified at 1254 and 1521 cm^{-1} arising from the COH and ring C=C vibrations, respectively [65]. These signals were proposed as being attributable to Y_Z structurally coupled with the Mn cluster. However, corresponding Tyr signals in other S-state transitions have not been reported yet, and thus further careful studies will be necessary for the final assignment of Tyr signals coupled to the Mn cluster.

It was asserted that bicarbonate bands were found at 1589 and 1365 cm^{-1} in the FTIR spectra of the OEC by comparing the spectra of PSII membranes in control medium, bicarbonate-depleted medium, and medium containing either unlabeled or ^{13}C-labeled bicarbonate at 1 mM concentration [66]. However, the measurements were performed with continuous illumination at room temperature, and thus the S-state transitions were not controlled. The reported spectra differ from any of the S-state spectra (Fig. 1), and seem to suffer severely from water vapor peaks as typical artifacts in FTIR difference spectra. Recent S-state measurements in the presence of unlabeled- or ^{13}C-labeled bicarbonate did not show any signals assignable to bicarbonate coupled to the OEC, although only the 1st-flash spectrum showed bicarbonate bands that arose from the non-heme iron center due to its preoxidation by ferricyanide [67].

4. Analysis of FTIR spectra by introducing perturbations to OEC

Although FTIR difference spectra of the S-state cycle contain a variety of information about the structures of S states and reactions during the S-state cycle, interpretation of the spectra to obtain specific information is often not straightforward even after bands are definitely assigned. One effective method to analyze the spectra is applying a certain perturbations to the OEC and then studying the effects on FTIR bands.

4.1. Ca^{2+} depletion and metal substitution

Ca^{2+} ion is an indispensable cofactor for oxygen evolution, and it is known that Ca^{2+}-depleted PSII undergoes the $S_1 \rightarrow S_2$ transition but higher transitions are blocked [68,69]. Ca^{2+} can be replaced with some other metal ions. Among them, only Sr^{2+} can restore the oxygen-evolving activity [68,69]. In X-ray structures [1,2], one Ca^{2+} ion is modeled to be located in the close vicinity to Mn ions. However, details of the structural relevance of the Ca^{2+} to the Mn cluster and the role of Ca^{2+} in the mechanism of oxygen-evolving reaction are not well understood. These problems can be studied by detecting the effects of Ca^{2+} depletion on the S_2/S_1 FTIR spectra and those of Sr^{2+} substitution on the spectra during the S-state cycle.

Noguchi et al. [18] measured an S_2/S_1 difference spectrum of Ca^{2+}-depleted PSII membranes of spinach and showed that Ca^{2+} depletion led to the disappearance of asymmetric and symmetric COO^- bands at 1587/1560 and 1364/1403 cm^{-1}, respectively, concomitant with reduced amide I intensities. In contrast, Kimura et al. [23,70–72] claimed by experiments using Chelex-treated buffer that Ca^{2+} depletion itself did not affect the carboxylate bands, but the presence of soluble chelators and/or K^+ caused the spectral changes via the interaction of chelators with the Mn ion and/or binding of K^+ to the Ca^{2+} site. Their "Ca^{2+}-depleted" PSII preparation also did not exhibit any appreciable changes in the Mn–O–Mn core vibrations at 606 cm^{-1} [72]. On the other hand, recent experiments by Taguchi and Noguchi [27] using a Ca^{2+}-depleted PSII sample, which contained neither soluble chelators nor K^+ ion but in the presence of Chelex-100 even during measurements, showed an S_2/S_1 spectrum very similar to the previous spectrum by Noguchi et al. [18] obtained using Ca^{2+}-depleted PSII in the presence of EDTA and a $K_4[Fe(CN)_6]/K_3[Fe(CN)_6]$ couple (Fig. 4). Thus,

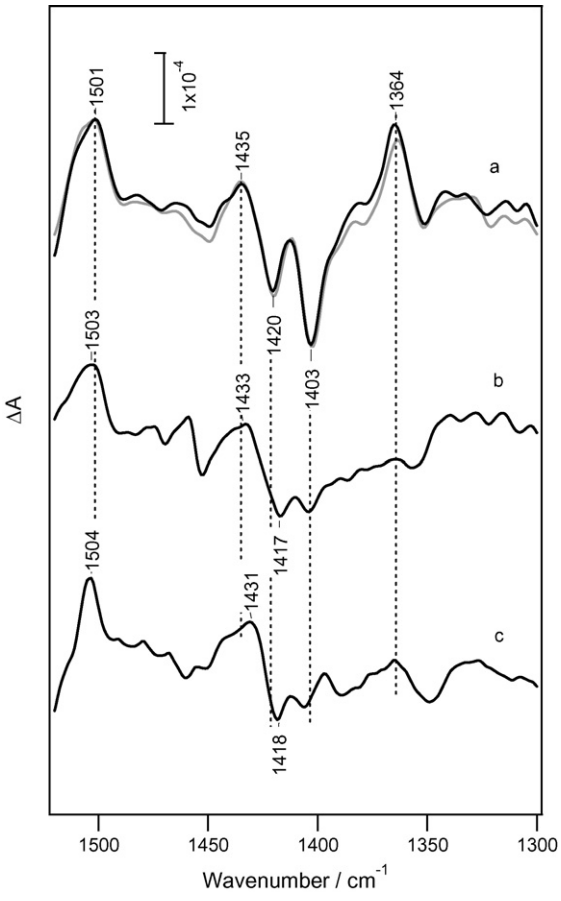

Fig. 4. S_2/S_1 difference spectra (symmetric COO^- region) of untreated (a, black line), Ca^{2+}-depleted (b, c), and Ca^{2+}-reconstituted (a, gray line) PSII membranes of spinach. The Ca^{2+}-depeted sample for spectrum b contained neither soluble chelators nor K^+ ions, but contained Chelelx-100 powder [27], while the Ca^{2+}-depleted sample for spectrum c contained 0.5 mM EDTA and 18/2 mM $K_4[Fe(CN)_6]/K_3[Fe(CN)_6]$ [18]. The spectra in a and b were obtained by subtracting a Q_A^-/Q_A spectrum from $S_2Q_A^-/S_1Q_A$ difference spectra measured at 10 °C in the presence of DCMU and the spectrum in c was obtained as a difference spectrum upon a single flash at 250 K.

the drastic FTIR changes were proven to be a pure effect of Ca^{2+} depletion and not due to chelators and K^+. Kimura et al. [23,70–72] adopted a NaCl wash as a method for Ca^{2+} depletion that removed the 23 and 17 kDa extrinsic proteins, whereas Noguchi et al. [18,27] used low-pH treatment that retained these proteins. It might be possible that absence of these extrinsic proteins facilitated the access of contaminating Ca^{2+} to the Mn cluster and hence effective chelators or metal substitution were necessary to remove Ca^{2+} from its binding site.

The drastic spectral changes by Ca^{2+} depletion provided solid evidence that Ca^{2+} is strongly coupled to the Mn cluster [18,27]. Noguchi et al. [18] interpreted the frequencies of the asymmetric and symmetric vibrations of Ca^{2+}-related carboxylate group (1560 and 1403 cm^{-1} in S_1 and 1587 and 1364 cm^{-1} in S_2) using a general correlation between the asymmetric–symmetric frequency gap ($\Delta\nu$) and the coordination structure of a carboxylate ligand [73,74]: (i) in unidentate coordination, $\Delta\nu$ is much greater (>∼200 cm^{-1}) than the ionic values (∼160 cm^{-1}), (ii) the chelating bidentate coordination exhibits a $\Delta\nu$ value (<∼100 cm^{-1}) significantly lower than the ionic values, and (iii) the $\Delta\nu$ value of a bridging bidentate structure is close to the ionic value (∼160 cm^{-1}). The large $\Delta\nu$ change from 157 to 223 cm^{-1} upon $S_1 \rightarrow S_2$ transition was attributed to a drastic coordination change from bridging bidentate to unidentate structure [18]. They proposed that the concerned carboxylate group bridged the Mn and Ca ions in the S_1 state and the coordination to Ca was disrupted upon S_2 formation, concomitant with conformational changes in polypeptide chains. It was further suggested that upon Ca^{2+} depletion, this carboxylate was released even from the Mn ion and hence the COO^- band changes by $S_1 \rightarrow S_2$ transition became silent together with diminished amide I intensities [18]. However, the carboxylate bands sensitive to Ca^{2+} depletion arise from neither the α-COO^- of D1-Ala344 [28,75] nor D1-Glu189 [37,47], which were modeled as bridging ligands between Ca and Mn in the X-ray structure by Loll et al. [2]. Thus, at present the straightforward interpretation of FTIR data is not consistent with the X-ray model. It could be possible that the concerned carboxylate ligand actually bridges two Mn ions which are strongly coupled with Ca^{2+} [27]. Also, Smith et al. [76] suggested that the general criteria to determine the coordination structures from $\Delta\nu$ values [73,74] do not hold over the range of Mn oxidation level shown in the S states.

In contrast to the drastic spectral changes by Ca^{2+} depletion, replacement of Ca^{2+} with Sr^{2+} showed rather similar features in the S_2/S_1 and S-state cycle spectra [29,70,72,75,77,78]. Upon a closer look, however, the spectra in the COO^- stretching regions were clearly perturbed, indicating that the ligand structure of the Mn cluster is somewhat different between Ca^{2+}-OEC and Sr^{2+}-OEC [29,70,72,75,77,78]. Suzuki et al. [78] suggested from the S-state cycle measurements of Sr^{2+}-subsituted PSII from *T. elongatus* and spinach that there are at least three carboxylate ligands whose structures are perturbed by Ca^{2+}/Sr^{2+} exchange. These carboxylate groups were suggested to be either direct ligands to the Ca^{2+} or ligands to the Mn ions that are strongly coupled to Ca^{2+}. Strickler et al. [75] showed that the symmetric COO^- bands of D1-Ala344 [(∼1339 or ∼ 1320)/∼1356 cm^{-1} in the S_2/S_1 states] were not altered by Sr^{2+} substitution, and thus concluded that the α-COO^- of D1-Ala344 is not a ligand to Ca^{2+}, but ligates a Mn ion. Chu et al. [57] showed that Sr^{2+} substitution upshifted the Mn–O–Mn band at 606 cm^{-1} in the S_2 state to ∼618 cm^{-1}, indicating that Sr^{2+} substitution causes a small structural perturbation that affects the bond length of the Mn–O–Mn cluster. This result was later confirmed by Kimura et al. [72]. When Ca^{2+} was replaced with K^+, Rb^+, Cs^+, and Ba^{2+}, carboxylate bands in the S_2/S_1 spectra were significantly modified and a strong negative peak at 1404 cm^{-1} diminished [70] similarly to the spectra of Ca^{2+}-depleted samples [18,27].

4.2. Cl^- depletion and anion substitution

Cl^- is also a cofactor essential to the OEC reactions. Upon Cl^- depletion, strong features in the amide I region of the S_2/S_1 spectra were mostly suppressed [79] concomitant with characteristic modification in the COO^- stretching bands [80]. The overall features were restored by addition of Br^-, I^- or NO_3^-, which can function in the Cl^- site, whereas replacement of Cl^- with F^- or CH_3COO^- resulted in marked suppression and distortion of both the carboxylate and amide bands [80]. The stretching vibrations of NO_3^- in the S_2/S_1 spectra of NO_3^--substituted PSII preparations were identified around 1400 cm^{-1} using $^{15}NO_3^-$ and $N^{18}O_3^-$ [80,81]. From comparisons of the observed NO_3^- frequencies with those of metal-bound NO_3^-, it was suggested that NO_3^- in the Cl^- site is coupled to the Mn-cluster, but not as a direct ligand. Cl^- depletion did not affect the Mn–O–Mn band at 606 cm^{-1}, which was consistent with an indirect interaction of Cl^- with the Mn cluster [72].

4.3. Ammonia treatment

Ammonia is an analogue of substrate water and an inhibitor of the oxygen-evolving reaction. Chu et al. [26] showed that the S_2/S_1 spectrum of NH_3-treated PSII exhibited a large upshift of the symmetric COO^- band at 1365 cm^{-1} in the S_2 state to 1379 cm^{-1}. This effect was seen at 250 K but not at 200 K. CH_3NH_2 also showed a similar but smaller spectral change, and the effects of amines were inverse proportional to their size. It was proposed that the shift of the 1365 cm^{-1} band is caused by the binding of NH_3 or a small amine to the site on the Mn cluster, which gives rise to the altered S_2 multiline EPR signal. This NH_3-induced effect was suppressed by the presence of ethylene glycol, whereas methanol was unable to compete with NH_3 upon binding to the Mn site [82]. The 1365 cm^{-1} COO^- band of the S_2 state was also sensitive to Ca^{2+} depletion [18,27] and Sr^{2+} substitution [75,78], suggestive of the proximity of the NH_3 binding site on the Mn cluster to the Ca^{2+} site.

4.4. Site-directed mutagenesis

Site-directed mutagenesis studies aiming at the assignment of carboxylate bands were already mentioned (Section 3.2). Here, other results are shortly summarized. Details of mutagenesis works including investigation using the FTIR difference technique are described in another review by Debus [83] in the same issue of this journal.

As mentioned above, the α-COO^- group of D1-Ala344 shows bands at (∼1339 or ∼1320)/∼1356 cm^{-1} in the S_2/S_1 spectrum of the core complexes of *Synechocystis* sp. PCC 6803 [28]. Interestingly, mutations at D1-Ala344 to Gly, Val, Asp, and Asn did not affect the α-COO^- bands but showed distinctive changes in several other COO^- bands [84,85]. The D1-Ala344Gly mutant also showed significant changes in the low-frequency spectra including the Mn–O–Mn core vibrations [84]. The Mn cluster core vibrations were also affected in the D1-Asp170His [44] and D1-Glu189Gln [47] mutants. These results indicate that D1-Ala344, D1-Asp170, and D1-Glu189 are structurally coupled to the Mn cluster and alterations of the side chains perturb the Mn core structure.

5. Analysis of interactions and reactions of water molecules

Interactions and reactions of substrate water or active water molecules in OEC were analyzed by FTIR measurements using isotopic water (D_2O, $H_2{}^{18}O$, and $D_2{}^{18}O$). Also, the processes of insertion of substrate water into the reaction cycle and proton release steps were studied by examining the effects of changing water content and pH, respectively, on the flash-induced spectra.

5.1. Hydrogen-bond interaction of an active water molecule

Noguchi and Sugiura [63] evaluated the intramolecular coupling of the two OH vibrations of the active water molecule, which showed the 3618/3585 cm^{-1} bands in the S_2/S_1 spectrum, by a decoupling experiment using a H_2O/D_2O (1:1) mixture (Fig. 5A). From the shifted peaks at 3616/3579 cm^{-1} (arising from the mixture of HOH and HOD), the downshifts by decoupling were estimated to be 4/12 cm^{-1}. These values are much smaller than 52 cm^{-1} of water in vapor, indicative of a considerably asymmetric structure of water, in which one OH is weakly and the other is strongly hydrogen bonded (Fig. 5B). The smaller coupling in the S_2 state than the S_1 state together with the upshift from 3585 to 3618 cm^{-1} indicates that the hydrogen bond asymmetry becomes more prominent upon S_2 formation (Fig. 5B). This structural change of water in the $S_1 \rightarrow S_2$ transition may facilitate the proton release in later steps. Fischer and Wydrzynski [53] performed quantum chemical calculations to estimate the coupling strength between the two OH stretches of water. From the above experimental shifts by decoupling [63], they predicted the frequencies of the strongly hydrogen-bonded OH stretching modes to be 3104 and 3392 cm^{-1} in the S_2 and S_1 states, respectively [53].

5.2. Interaction between a carboxylate group and a water molecule

An asymmetric COO^- band at ∼1561 cm^{-1} in the S_2/S_1 difference spectrum of PSII membranes of spinach was found to undergo a large upshift by ∼18 cm^{-1} upon H_2O/D_2O exchange [86]. A similar upshift was observed in the 1st-flash spectrum ($S_1 \rightarrow S_2$) of *T. elongatus* core complexes and the counter-band

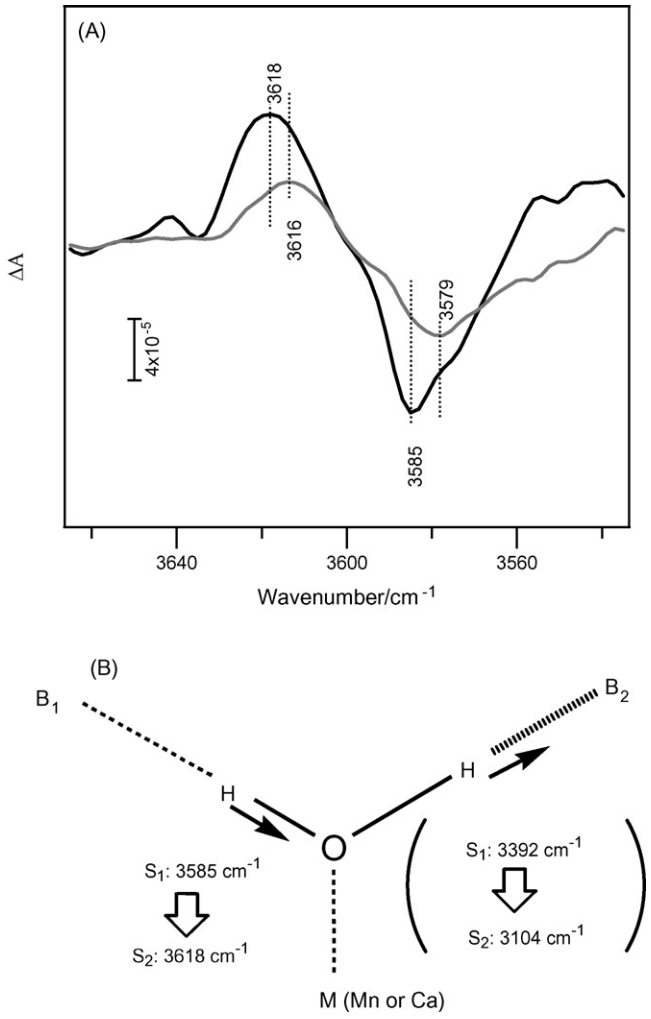

Fig. 5. (A) The OH stretching bands of active water molecule in the S_2/S_1 difference spectrum of *T. elongatus* core complexes in H_2O (black line) and in H_2O/D_2O (1:1) (gray line) [63]. The spectra were recorded at 250 K. (B) The proposed structure of the water molecule detected by FTIR. B_1 and B_2 represent hydrogen-bond acceptors. Arrows indicate the directions of structural changes upon the $S_1 \rightarrow S_2$ transition. The frequencies of the OH bond weakly hydrogen-bonded with B_1 are experimental values and those of the OH bond strongly hydrogen-bonded with B_2 are the values predicted using quantum chemical calculations [53].

was found in the 4th-flash spectrum ($S_0 \rightarrow S_1$) [35]. It was proposed from FTIR measurements of model carboxylate compounds with different types of hydrogen-bonding interaction that this H/D sensitive band arose from the asymmetric COO^- vibration coupled with a H_2O bending mode in a carboxylate ligand hydrogen-bonded with a water molecule bound to the Mn ion [86]. Quantum chemical calculations by Fisher and Wydrzynski [53] reproduced the coupling of the asymmetric COO^- vibration with the bending vibration of a hydrogen-bonded water molecule. However, their results showed that a deuterium-induced upshift requires rather symmetric interactions of the COO^- group. Further studies using FTIR measurements of model compounds together with theoretical calculations are necessary to determine the configuration of the COO^- and water interaction that were revealed by the deuteration effect on the COO^- band.

5.3. Substrate insertion and proton release

Dependency on the substrate content in the water oxidizing reaction was analyzed as dehydration effects on the efficiencies of individual S-state transitions [34]. The water content was controlled by changing the relative humidity in the IR cell. Upon decreasing the water content (i.e., the amount of substrate), the efficiencies of the $S_2 \rightarrow S_3$ and $S_3 \rightarrow S_0$ transitions decreased faster than those of the $S_1 \rightarrow S_2$ and $S_0 \rightarrow S_1$ transitions. This result suggests that insertion of water molecules into the OEC via water pathways takes place mainly in the $S_2 \rightarrow S_3$ and/or $S_3 \rightarrow S_0$ transitions. Note that such water insertion into the OEC does not necessarily represent binding of the substrate water to the Mn cluster.

Proton release reactions of substrate water were investigated by examining the pH dependence of the S-state transition efficiencies. Flash-induced FTIR spectra were measured with *T. elongatus* core complexes in buffers at various pHs [87]. Whereas the $S_1 \rightarrow S_2$ transition probability was independent of pH throughout the pH range of 3.5–9.5, the other three transitions were all inhibited at acidic pH. The apparent pK_a values were estimated as 3.6 ± 0.2, 4.2 ± 0.3, and 4.7 ± 0.5 for the $S_2 \rightarrow S_3$, $S_3 \rightarrow S_0$, and $S_0 \rightarrow S_1$ transitions, respectively, which were in good agreement with the previous estimations for spinach PSII membranes by EPR spectroscopy [88]. These observations are consistent with the view that proton release from substrate water takes place at the three transitions other than $S_1 \rightarrow S_2$.

6. Concluding remarks and perspectives

FTIR studies on OEC have been extensively performed for the past 15 years and light-induced FTIR difference spectroscopy has become one of the major techniques in investigation of photosynthetic oxygen evolution. Reported spectra have provided a variety of structural information on the constituents of OEC, i.e., the Mn-cluster core, amino acid ligands, polypeptide backbones, and active water molecules. The reaction processes have been examined by detecting flash-dependent spectral changes. Definite assignments of the observed bands to specific amino acid residues are urgent for identification of ligands to the Mn and Ca ions, and thus further investigations in combination with site-directed mutagenesis and selective isotope substitutions will be necessary. Also, identification of substrate water molecules and their interactions to specific amino acids are crucial for understanding the mechanism of water oxidation. As the resolution of the X-ray crystallographic structure is improved, complementary structural information and reaction analysis by FTIR will become more important. Thus, FTIR difference spectroscopy will play a key role in future investigation of photosynthetic oxygen evolution toward full understanding of its molecular mechanism.

Acknowledgements

The author thanks Professor Richard Debus for critical reading of the manuscript. This study was supported by Grant-in-Aid for Scientific Research (17GS0314 and 18570145) from the Ministry of Education, Science, Sports, Culture and Technology, and by Special Research Project "NanoScience" at the University of Tsukuba.

References

[1] K.N. Ferreira, T.M. Iverson, K. Maghlaoui, J. Barber, S. Iwata, Science 303 (2004) 1831.
[2] B. Loll, J. Kern, W. Saenger, A. Zouni, J. Biesiadka, Nature 438 (2005) 1040.
[3] J. Yano, J. Kern, K.D. Irrgang, M.J. Latimer, U. Bergmann, P. Glatzel, Y. Pushkar, J. Biesiadka, B. Loll, K. Sauer, J. Messinger, A. Zouni, V.K. Yachandra, Proc. Natl. Acad. Sci. U.S.A. 102 (2005) 12047.
[4] M. Grabolle, M. Haumann, C. Muller, P. Liebisch, H. Dau, J. Biol. Chem. 281 (2006) 4580.
[5] W. Mäntele, Trends Biochem. Sci. 18 (1993) 197.
[6] R. Vogel, F. Siebert, Curr. Opin. Chem. Biol. 4 (2000) 518.
[7] C. Zscherp, A. Barth, Biochemistry 40 (2001) 1875.
[8] M. Seibert, T.M. Cotton, FEBS Lett. 182 (1985) 34.
[9] A. Cua, D.H. Stewart, M.J. Reifler, G.W. Brudvig, D.F. Bocian, J. Am. Chem. Soc. 122 (2000) 2069.
[10] T. Noguchi, T. Ono, Y. Inoue, Biochemistry 31 (1992) 5953.
[11] W. Hillier, G.T. Babcock, Biochemistry 40 (2001) 1503.
[12] T. Noguchi, M. Sugiura, Biochemistry 40 (2001) 1497.
[13] H.-A. Chu, W. Hillier, N.A. Law, G.T. Babcock, Biochim. Biophys. Acta 1503 (2001) 69.
[14] T. Noguchi, Photosynth. Res. 91 (2007) 59.
[15] T. Noguchi, C. Berthomieu, in: T. Wydrzynski, K. Satoh (Eds.), Photosystem II: The Light-Driven Water:Plastoquinone Oxidoreductase, Springer, Dordrecht, The Netherlands, 2005, p. 367.
[16] R. Hienerwadel, C. Berthomieu, Biochemistry 34 (1995) 16288.
[17] T. Noguchi, Y. Inoue, J. Biochem. 118 (1995) 9.
[18] T. Noguchi, T. Ono, Y. Inoue, Biochim. Biophys. Acta 1228 (1995) 189.
[19] T. Noguchi, T. Ono, Y. Inoue, Biochim. Biophys. Acta 1143 (1993) 333.
[20] K. Onoda, H. Mino, Y. Inoue, T. Noguchi, Photosynth. Res. 63 (2000) 47.
[21] H. Zhang, G. Fischer, T. Wydrzynski, Biochemistry 37 (1998) 5511.
[22] H.-A. Chu, M.T. Gardner, J.P. O'Brien, G.T. Babcock, Biochemistry 38 (1999) 4533.
[23] Y. Kimura, T. Ono, Biochemistry 40 (2001) 14061.
[24] A. Remy, J. Niklas, H. Kuhl, P. Kellers, T. Schott, M. Rogner, K. Gerwert, Eur. J. Biochem. 271 (2004) 563.
[25] C. Berthomieu, E. Nabedryk, W. Mäntele, J. Breton, FEBS Lett. 269 (1990) 363.
[26] H.-A. Chu, Y.-W. Feng, C.-M. Wang, K.-A. Chiang, S.-C. Ke, Biochemistry 43 (2004) 10877.
[27] Y. Taguchi, T. Noguchi, Biochim. Biophys. Acta, in press.
[28] H.-A. Chu, W. Hillier, R.J. Debus, Biochemistry 43 (2004) 3152.
[29] B.A. Barry, C. Hicks, A. De Riso, D.L. Jenson, Biophys. J. 89 (2005) 393.
[30] J.J. Steenhuis, B.A. Barry, J. Phys. Chem. B 101 (1997) 6652.
[31] J.J. Steenhuis, R.S. Hutchison, B.A. Barry, J. Biol. Chem. 274 (1999) 14609.
[32] T. Okubo, T. Noguchi, Spectrochim. Acta A 66 (2007) 863.
[33] H.-A. Chu, W. Hillier, N.A. Law, H. Sackett, S. Haymond, G.T. Babcock, Biochim. Biophys. Acta 1459 (2000) 528.
[34] T. Noguchi, M. Sugiura, Biochemistry 41 (2002) 2322.
[35] T. Noguchi, M. Sugiura, Biochemistry 41 (2002) 15706.
[36] G. Socrates, Infrared Characteristic Group Frequencies, John Wiley & Sons, Chichester, 1994.
[37] M.A. Strickler, W. Hillier, R.J. Debus, Biochemistry 45 (2006) 8801.
[38] W.K. Surewicz, H.H. Mantsch, Biochim. Biophys. Acta 952 (1988) 115.
[39] T. Noguchi, M. Sugiura, Y. Inoue, in: K. Itoh, M. Tasumi (Eds.), Fourier Transform Spectroscopy, Waseda University Press, Tokyo, 1999, p. p. 459.
[40] T. Noguchi, M. Sugiura, Biochemistry 42 (2003) 6035.
[41] Y. Kimura, N. Mizusawa, A. Ishii, T. Yamanari, T. Ono, Biochemistry 42 (2003) 13170.

[42] T. Yamanari, Y. Kimura, N. Mizusawa, A. Ishii, T. Ono, Biochemistry 43 (2004) 7479.
[43] Y. Kimura, N. Mizusawa, T. Yamanari, A. Ishii, T. Ono, J. Biol. Chem. 280 (2005) 2078.
[44] H.-A. Chu, R.J. Debus, G.T. Babcock, Biochemistry 40 (2001) 2312.
[45] R.J. Debus, M.A. Strickler, L.M. Walker, W. Hillier, Biochemistry 44 (2005) 1367.
[46] M.A. Strickler, L.M. Walker, W. Hillier, R.D. Britt, R.J. Debus, Biochemistry 46 (2007) 3151.
[47] Y. Kimura, N. Mizusawa, A. Ishii, S. Nakazawa, T. Ono, J. Biol. Chem. 280 (2005) 37895.
[48] C. Berthomieu, A. Boussac, W. Mäntele, J. Breton, E. Nabedryk, Biochemistry 31 (1992) 11460.
[49] T. Noguchi, Y. Inoue, X.-S. Tang, Biochemistry 38 (1999) 10187.
[50] K. Hasegawa, T. Ono, T. Noguchi, J. Phys. Chem. B 104 (2000) 4253.
[51] K. Hasegawa, T. Ono, T. Noguchi, J. Phys. Chem. A 106 (2002) 3377.
[52] A. Toyama, K. Ono, S. Hashimoto, H. Takeuchi, J. Phys. Chem. A 106 (2002) 3403.
[53] G. Fischer, T. Wydrzynski, J. Phys. Chem. B 105 (2001) 12894.
[54] Y. Kimura, N. Mizusawa, A. Ishii, T. Ono, Biochemistry 44 (2005) 16072.
[55] G.J. Hawkins, R. Hunneman, M.T. Gardner, G.T. Babcock, Infrared Phys. Technol. 39 (1998) 297.
[56] H.-A. Chu, M.T. Gardner, W. Hillier, G.T. Babcock, Photosynth. Res. 66 (2000) 57.
[57] H.-A. Chu, H. Sackett, G.T. Babcock, Biochemistry 39 (2000) 14371.
[58] H. Visser, C.E. Dube, W.H. Armstrong, K. Sauer, V.K. Yachandra, J. Am. Chem. Soc. 124 (2002) 11008.
[59] A. Cua, J.S. Vrettos, J.C. de Paula, G.W. Brudvig, D.F. Bocian, J. Biol. Inorg. Chem. 8 (2003) 439.
[60] K. Hasegawa, T. Ono, Bull. Chem. Soc. Jpn. 79 (2006) 1025.
[61] H.-A. Chu, W. Hillier, N.A. Law, G.T. Babcock, Proceedings of the 12th International Congress on Photosynthesis, CSIRO Publishing, Collingwood, 2001, p. S13.
[62] Y. Kimura, A. Ishii, T. Yamanari, T. Ono, Biochemistry 44 (2005) 7613.
[63] T. Noguchi, M. Sugiura, Biochemistry 39 (2000) 10943.
[64] G. Zundel, J. Mol. Struct. 177 (1988) 43.
[65] T. Noguchi, Y. Inoue, X.-S. Tang, Biochemistry 36 (1997) 14705.
[66] I. Yruela, S.I. Allakhverdiev, J.V. Ibarra, V.V. Klimov, FEBS Lett. 425 (1998) 396.
[67] C. Aoyama, H. Suzuki, M. Sugiura, T. Noguchi, Plant Cell Physiol. 48 (Suppl.) (2007) s75.
[68] R.J. Debus, Biochim. Biophys. Acta 1102 (1992) 269.
[69] H.J. van Gorkom, C.F. Yocum, in: T. Wydrzynski, K. Satoh (Eds.), Photosystem II: The Light-Driven Water:Plastoquinone Oxidoreductase, Springer, Dordrecht, The Netherlands, 2005, p. 307.
[70] Y. Kimura, K. Hasegawa, T. Ono, Biochemistry 41 (2002) 5844.
[71] Y. Kimura, T. Ono, J. Inorg. Biochem. 97 (2003) 231.
[72] Y. Kimura, K. Hasegawa, T. Yamanari, T. Ono, Photosynth. Res. 84 (2005) 245.
[73] G.B. Deacon, R.J. Phillips, Coord. Chem. Rev. 33 (1980) 227.
[74] K. Nakamoto, Infrared and Raman Spectra of Inorganic and Coordination Compounds, part B, 5th ed., John Wiley & Sons, New York, 1997, p. 59.
[75] M.A. Strickler, L.M. Walker, W. Hillier, R.J. Debus, Biochemistry 44 (2005) 8571.
[76] J.C. Smith, E. Gonzalez-Vergara, J.B. Vincent, Inorg. Chim. Acta 255 (1997) 99.
[77] A. De Riso, D.L. Jenson, B.A. Barry, Biophys. J. 91 (2006) 1999.
[78] H. Suzuki, Y. Taguchi, M. Sugiura, A. Boussac, T. Noguchi, Biochemistry 45 (2006) 13454.
[79] T. Noguchi, T. Ono, Y. Inoue, in: P. Mathis (Ed.), Photosynthesis: From Light to Biosphere, II, Kluwer Academic Publishers, Dordrecht, The Netherlands, 1995, p. 235.
[80] K. Hasegawa, Y. Kimura, T. Ono, Biochemistry 41 (2002) 13839.
[81] K. Hasegawa, Y. Kimura, T. Ono, Biophys. J. 86 (2004) 1042.
[82] C.-H. Fang, K.-A. Chiang, C.-H. Hung, K. Chang, S.-C. Ke, H.-A. Chu, Biochemistry 44 (2005) 9758.
[83] R.J. Debus, Coord. Chem. Rev. 252 (2008) 244.
[84] N. Mizusawa, Y. Kimura, A. Ishii, T. Yamanari, S. Nakazawa, H. Teramoto, T. Ono, J. Biol. Chem. 279 (2004) 29622.
[85] N. Mizusawa, T. Yamanari, Y. Kimura, A. Ishii, S. Nakazawa, T. Ono, Biochemistry 43 (2004) 14644.
[86] T. Noguchi, T. Ono, Y. Inoue, Biochim. Biophys. Acta 1232 (1995) 59.
[87] H. Suzuki, M. Sugiura, T. Noguchi, Biochemistry 44 (2005) 1708.
[88] G. Bernát, F. Morvaridi, Y. Feyziyev, S. Styring, Biochemistry 41 (2002) 5830.